

Direct determination of Pb isotope ratios in archaeological materials by coupling Liquid Chromatography to Multicollector ICP-MS.

Pelayo Alvarez Penanes¹, Mariella Moldovan¹, Alfredo Mederos², Pablo Martín-Ramos³, J. Ignacio García Alonso^{1*}

¹Department of Physical and Analytical Chemistry. Faculty of Chemistry. University of Oviedo. Julian Claveria 8, 33006, Oviedo, Spain

²Department of Prehistory and Archaeology, Faculty of Philosophy and Letters, Autonomous University of Madrid, Campus of Cantoblanco, 28049 Madrid, Spain

³Escuela Politécnica Superior, Universidad de Zaragoza. Carretera de Cuarte s/n, 22071-Huesca, Spain

*e-mail: jiga@uniovi.es

Abstract

A procedure for the determination of Pb isotope ratios by coupling Liquid Chromatography to a multicollector ICP-MS has been developed. The procedure allows the direct injection of samples after dissolution without resorting to time-consuming off-line separation procedures. The separation of Pb from concomitant elements is carried out by anionic exchange as ethylenediamine tetraacetic acid (EDTA) chelates using EDTA and ammonium nitrate as mobile phase. A flow injection system allows the injection of NIST 981 Pb isotopic standard, before and after the Pb peak from the sample, and the on-line addition of Tl for mass bias correction and bracketing. The procedure was validated by injecting NIST 981 in the chromatographic system and by comparing the results for real samples with the classical off-line separation procedure using Pb spec resins. The optimised procedure was applied to archaeological samples containing different concentrations of Pb. It was observed that the only limitation to the accuracy of the procedure was the concentration of Pb in the samples as no preconcentration is performed. Solid archaeological samples containing at least 500 $\mu\text{g g}^{-1}$ of Pb can be studied using the proposed procedure.

1. Introduction

Isotope ratio measurements are a powerful tool in numerous scientific fields such as geochronology¹, archaeometry^{2,3,4,5}, food authentication^{6,7}, metabolism^{8,9} and environmental pollution monitoring^{10,11}, to mention only a few areas of interest. Amongst all the heavy elements suitable to isotopic analysis, lead is the one showing the largest isotopic variability in nature¹². Lead has four stable isotopes (²⁰⁴Pb, ²⁰⁶Pb, ²⁰⁷Pb and ²⁰⁸Pb), three of them being the end products of the radioactive decay of the long-lived parent nuclides ²³²Th (to ²⁰⁸Pb), ²³⁵U (to ²⁰⁷Pb) and ²³⁸U (to ²⁰⁶Pb). This variable isotopic composition can be applied, for example, in

1
2
3 archaeometry to unravel the provenance of archaeological artefacts, by comparison to the data
4 available for the different mines around the world⁵.

6
7 During the 20th century, Thermal Ionization Mass Spectrometry (TIMS) was the method of
8 choice for high precision isotope ratio determinations. The complex sample preparation
9 procedures required for TIMS measurements were expected to be minimized or eliminated with
10 the advent of Multicollector Inductively Coupled Plasma Mass Spectrometry (MC-ICP-MS)
11 instruments in 1992¹³. Using these instruments, the combination of the inductively coupled
12 plasma ion source with the simultaneous detection of the ions by means of an array of Faraday
13 cups, it was expected to reduce both sample preparation and measuring time while increasing
14 elemental coverage and sensitivity. Although this is true to a certain extent, for optimum results
15 to be obtained it is still necessary to chemically isolate the target element from the concomitant
16 matrix, a process that involves off-line separations using resins and/or chelating agents^{7,14,15}.
17 Additionally, the analysis of an isotopically certified reference material both before and after the
18 sample (standard-sample-standard bracketing procedure), with careful matching of the signals
19 on both the standard and the sample, is paramount in order to achieve the best precision and
20 accuracy. Another problem arises when sample availability is a limiting factor, such as for
21 archaeological artefacts where taking minimum amounts of sample is usually required. Hence,
22 we propose an alternative methodology in which the separation of lead from the interfering
23 elements and the correction of mass discrimination, both externally (with TI) and via bracketing
24 (with the certified reference material) is performed on-line.

25
26 The hyphenation of different separation techniques to the multicollector instrument is
27 extensively described in the literature^{16,17,18,19,20}, particularly for liquid chromatography^{21,22,23,24}.
28 This coupling implies working with transient signals, a more demanding task in comparison to
29 the classical approach with constant nebulization of the sample and continuous signals. To
30 circumvent this problem, a very elegant way to calculate isotope ratios irrespective of the
31 sample introduction mode is to plot the different signals obtained for the different isotopes^{25,26}.
32 The isotope ratio would be the slope of the resulting line. In the case of constant signals, the line
33 is defined to “ $y=bx$ ”; whilst for transient signals, the line is adjusted to “ $y=a+bx$ ”, to correct for
34 the background contribution. In both cases, the uncertainty of the isotope ratio is the standard
35 error of the slope²⁶.

36
37 On account of this, we propose an alternative procedure for the fast, precise and accurate
38 determination of lead isotope ratios in archaeological samples containing at least 500 $\mu\text{g g}^{-1}$ of
39 Pb. The combination of a flow injection analysis system (for mass discrimination correction)
40 with liquid chromatography (for the separation of lead from the rest of the elements present in
41 the sample) allows the rapid determination of lead isotope ratios without compromising the
42 precision and accuracy necessary in this type of analysis.

2. Experimental

2.1. Reagents and materials

Pro analysi nitric acid (14 mol L⁻¹) and *pro analysi* hydrochloric acid (12 mol L⁻¹) were purchased from Merck (Darmstadt, Germany). Both acids were further purified by sub-boiling distillation using a Savillex PFA apparatus (Savillex, Minnetonka, MN, USA). *Pro analysi* ammonium oxalate monohydrate (NH₄)₂ C₂O₄·H₂O and *pro analysi* ammonium nitrate were purchased from Merck (Darmstadt, Germany). Ethylenediamine tetraacetic acid (EDTA) was purchased from Probus S.A. (Badalona, Spain). Ultrapure water with a resistivity >18.2 MΩ cm was obtained from a Milli-Q Gradient A10 water purification system (Millipore, Molsheim, France) and was used for mobile phase preparation and for diluting concentrated acids. Tl and As standards were purchased from Merck (Darmstadt, Germany). Cu standard was purchased from Sigma-Aldrich (St. Louis, MO, USA). Zn standard was purchased from Absolute Standards INC (Hamden, CT, USA). Sn standard was purchased from High Purity Standards (Charleston, SC, USA). Certified reference material SRM 981 (Pb isotopic standard) from the National Institute for Standards and Technology, NIST (Gaithersburg, MD, USA) was used for standard-sample-standard bracketing.

Sample digestion was performed in flat-bottom screw cap Teflon (PFA) beakers (Savillex, AHF Analysentechnik, Tübingen, Germany). Lead separation was performed using a Pb specTM resin purchased from TrisKem International (Bruz, France) loaded into a Bio-Rad polypropylene column. After each digestion, beakers were cleaned in a three-step protocol consisting of 24 h at 110 °C in HCl 6 mol L⁻¹, 24 h at 110 °C in HNO₃ 7 mol L⁻¹ and 24 h at 110 °C in H₂O Milli-Q. Flow injection connectors and tubing were obtained from Scharlab S. L. (Barcelona, Spain).

2.2. Instrumentation

All chromatographic separations were accomplished using a Dionex DX-120 ion chromatograph (Sunnyvale, CA, USA) and an anion exchange column (Ion Pac AS9-HC 4x250 mm), with an injection loop of 100 µl. Chromatographic separation between different elements was assessed using a Q-ICP-MS Agilent 7500 ce (Agilent Technologies, Tokyo, Japan).

For the introduction of the certified reference material solution before and after the sample, a *Diba Omnifit* 6-way low-pressure injection valve, fitted with an injection loop of 150 µl, was purchased from Scharlab S. L. (Barcelona, Spain).

FIA optimisation, MC-ICP-MS parameters optimisation and sample measurements were performed with a Thermo Scientific Neptune Plus multicollector ICP-MS instrument (Thermo

Scientific, Bremen, Germany) equipped with a combined (cyclonic/double-pass) spray chamber and a 1-mL *Conikal* glass nebuliser (Glass Expansion, Weilburg, Germany). Optimum operation conditions are summarized in **Table 1**.

2.3. Samples investigated

In this study we evaluated archaeological samples containing a large interval of Pb concentrations (from low $\mu\text{g g}^{-1}$ to percentage levels) obtained in different archaeological excavations. Details of the origin of the samples can be found elsewhere²⁷. The concentration of Pb in those samples (semiquantitative analysis with one point calibration) is given in **Table 2**. For the samples containing low Pb concentrations there was also limited availability and the weight taken was in all cases lower than the recommended weight of 100 mg.

2.4. Sample preparation

Between 10 and 100 mg of sample (depending on availability) were treated with 8 ml of *aqua regia* and heated at 110 °C during 24 h. After complete digestion of the sample and subsequent evaporation to dryness, samples were dissolved in 2 ml of 1 mol L⁻¹ HNO₃. An aliquot of 1 mL was subjected to an off-line separation procedure described elsewhere^{14,28}, where Pb is separated from the concomitant sample matrix by using a resin specific for Pb isolation. This protocol will be hereafter referred as conventional approach. A second aliquot of 100 μL was again evaporated to dryness and redissolved in 1 mL 50 mmol L⁻¹ EDTA and heated at 110 °C during 30 minutes. This protocol will be henceforth denoted as the online approach.

2.5. Analytical procedure for Pb isotope ratio measurements

The sample was injected in the HPLC-MC-ICP-MS system and, immediately, the NIST 981 standard injected in the Flow Injection Valve. Then, after the elution of Pb from the chromatographic column, a second injection of the NIST 981 standard was carried out. The whole acquisition procedure took 10 minutes. After acquisition, data treatment consisted of the measurement of the Pb isotope ratios for the three peaks using the linear regression slope procedure, the internal correction of mass bias using the Tl isotope ratios measured for each peak and the final bracketing of the sample Pb isotope ratios using the average of the data for the two NIST standards injected before and after the elution of Pb from the chromatographic column.

2.6. Calculation of total combined uncertainties.

1
2
3 Combined uncertainties for single measurements were calculated taking into account the
4 uncertainties of all measurement steps including the uncertainties of the measured isotope ratios
5 in the sample, the uncertainty in the Tl isotope ratio for mass bias correction and the
6 uncertainties of the measured and certified NIST 981 Pb isotopic standard. The experimental
7 uncertainties were taken directly from the standard uncertainties in the slope of the lineal
8 regression procedure. The theoretical uncertainties of the reference material were calculated by
9 dividing the expanded uncertainties given in the certificate by the coverage factor of 2. Final
10 combined uncertainties, u_f , for triplicate measurements were calculated using the equation:

$$u_f = \sqrt{(u_t)^2 + (u_i)^2} \quad (1)$$

11
12
13
14
15
16
17
18
19
20
21
22 Where u_t is the standard uncertainty of the triplicate measurement (the standard deviation of the
23 three independent measurements divided by the square root of 3) and u_i is the quadratic mean of
24 the combined standard uncertainties of the three single measurements performed:

$$u_i = \sqrt{((u_1)^2 + (u_2)^2 + (u_3)^2)/3} \quad (2)$$

25
26
27
28
29
30
31
32
33 It is worth noting here that the major source of uncertainty was always the theoretical
34 uncertainty of the reference material.

3. Results and discussion

3.1. Chromatographic separation

35
36
37
38
39
40
41
42
43
44 The objective of this study was to develop a chromatographic procedure in which the different
45 metals that could be present at high concentration levels in archaeological artefacts (arsenical
46 copper, bronze, lead pipes, etc.) could be separated from each other. For example, we have
47 observed that high levels of Cu have a detrimental effect on Pb isotope ratios (see Figure S1 in
48 the Supplementary Information) and both elements need to be separated. Previous work in our
49 laboratory on the separation of lanthanides²⁹ showed that anion chromatography of anionic
50 EDTA complexes was a suitable separation procedure. In order to optimise the separation of Pb
51 from potential interfering elements present in the samples, 10 $\mu\text{g L}^{-1}$ solutions of different
52 metals (Pb, Sn, As, Zn, Fe and Cu) were prepared in the different mobile phases under study,
53 containing varying amounts of ammonium nitrate (5-100 mmol L^{-1}) and a fixed concentration of
54
55
56
57
58
59
60

1
2
3 EDTA (5 mmol L⁻¹). The pH of the different mobile phases was adjusted to 6.2 with an
4 ammonia solution.
5

6 The best separation was achieved for a mobile phase 25 mmol L⁻¹ NH₄NO₃/5 mmol L⁻¹ EDTA,
7 as can be seen in **Figure 1**, in which Pb appears perfectly separated from the rest of the metals
8 present in the solution. It is relevant that Cu elutes after Pb, since copper is the major
9 component in the vast majority of archaeological samples of interest. In this way we do not
10 have to worry about the tailing from the Cu peak hindering the measurement of Pb isotope
11 ratios, as it could happen if Cu elution took place before Pb.
12
13
14
15
16
17

18 3.2. Set-up for LC-MC-ICP-MS Pb measurements

19 Once the chromatographic separation has been achieved, the HPLC was coupled on-line to the
20 multicollector instrument through the inlet of the concentric nebulizer as shown in **Figure 2**.
21 Thallium for mass bias correction (prepared using the mobile phase) and the carrier for the Pb
22 NIST reference material (ultrapure water) were introduced post-column by means of a
23 peristaltic pump. The reference material used for the bracketing (NIST 981) was injected prior
24 and after the sample with the aid of a low-pressure 6-way valve. Flow rates for the three lines
25 were 0.8 (HPLC), 0.1 (Tl) and 0.1 (Pb NIST) mL/min respectively. The waste from the cyclonic
26 spray chamber was pumped away using the same peristaltic pump.
27
28
29
30
31
32
33

34 3.3. Optimisation and evaluation of the on-line procedure

35 When measuring constant signals with a multicollector instrument, long integration times (ca. 4
36 s) are the preferred option. On the other hand, short integration times (ca. 0.1 s) are
37 recommended when dealing with fast-changing transient peaks³⁰, in order to better follow the
38 peak profiles. In this approach, both types of signals are present at the same time: a constant
39 signal for thallium and a transient signal for lead (HPLC and reference material for the
40 bracketing and the sample). Hence, it is expected that a compromise integration time will
41 provide the best results.
42
43
44
45
46
47

48 To test this hypothesis, solutions of the NIST SRM 981 at different concentration levels (250,
49 500 and 1000 µg L⁻¹) were injected in the HPLC system in triplicate, using different integration
50 times (from 0.1 to 4.2 s) and adjusting the number of cycles accordingly to obtain a final
51 chromatographic time of 10 minutes in all cases. The concentration of post-column Tl was kept
52 constant at 500 µg L⁻¹. The relative combined uncertainties (%) obtained for each isotope ratio,
53 concentration and integration time are summarised in **Table 3**. These data are expressed as
54 combined uncertainties taking into account the uncertainties of the isotope ratios for each
55 chromatogram, corrected for mass bias using the Tl isotope ratios, and the standard error of the
56
57
58
59
60

1
2
3 average triplicate injections (equation 2). The best results were obtained for an integration time
4 of 1 s at all concentration levels tested, particularly for the case of $^{206}\text{Pb}/^{204}\text{Pb}$, involving the
5 least abundant Pb isotope (^{204}Pb). For the other ratios evaluated, the uncertainties were not so
6 critically affected by the integration time. Hence, an integration time of 1 s (and 600 cycles, for
7 a final chromatogram of 10 minutes) was selected for the measurement of the samples.
8
9

10
11 In all cases, the whole peak was considered to calculate the isotope ratios by the linear
12 regression slope procedure in order to avoid possible fractionation effects in the column and the
13 system. For the particular case of the selected integration time (1 s), 125 data points (cycles)
14 were sufficient to include the background before and after the signal of the samples and/or
15 standards. In each case, only the thallium signal encompassing those 125 points was taken into
16 account for mass bias correction using the Russell equation:
17
18
19

$$R_{\text{corr}} = R_{\text{exp}} \left(\frac{m_2}{m_1} \right)^f \quad (3)$$

20
21 where R_{corr} is the true ratio in the sample, R_{exp} is the uncorrected value obtained in the
22 measurement run, m_1 and m_2 refer to the masses of the isotopes under study, and f is the
23 correction factor, calculated using a certified isotopic standard³¹.
24
25

26 Data treatment was performed off-line by means of an Excel file and using the procedure
27 described²⁵⁻²⁶. Isotope ratios were calculated using the function LINEST, and as it was
28 previously mentioned, continuous signals (Tl) were adjusted to “ $y=bx$ ”, and transient signals
29 (Pb) were adjusted to “ $y=a+bx$ ”. The slope thus obtained is the isotope ratio, and the standard
30 error of the measurement is the standard deviation of the slope.²⁶
31
32

33 In order to check which concentrations for the post-column Tl and the bracketing Pb NIST
34 resulted in the best results in terms of precision, a real sample was “simulated” preparing a
35 standard containing $500 \mu\text{g L}^{-1}$ of Pb NIST 981 and 500mg L^{-1} of Cu, using the mobile phase as
36 solvent. Different concentrations of post-column Tl and bracketing Pb ($250, 500$ and $1000 \mu\text{g L}^{-1}$)
37 were tested, and for each concentration of post-column Tl and Pb bracketing, the standard
38 solution was measured in triplicate. As shown in **Table 4** the best results in terms of relative
39 combined uncertainties were obtained for a Tl concentration of $1000 \mu\text{g L}^{-1}$ and a Pb
40 concentration of $500 \mu\text{g L}^{-1}$. Please note that in comparison with Table 3 the relative
41 uncertainties in Table 4 are ca. 10 times worse for Pb. This is due to the fact that additional
42 sources of uncertainty were taken into account here such as the experimental uncertainty of the
43 NIST 981 injections both before and after the sample and the theoretical uncertainty of the Pb
44 isotope ratios in the NIST standard. The combined uncertainties shown in Table 4 are now close
45 to what could be expected for the analysis of real samples. For the Tl measurements only the
46 experimental uncertainties are given and those are similar both in Tables 3 and 4.
47
48
49
50
51
52
53
54
55
56
57
58
59
60

1
2
3 In MC-ICP-MS measurements, signal-matching between samples and standards is of the utmost
4 importance in order to attain the best precision and accuracy. Unfortunately, in this approach it
5 is not possible to perfectly adjust the concentration of the sample beforehand. Hence, it is
6 necessary to test whether the concentration of Pb in the sample injected has an effect on the
7 quality of the measurements in terms of bias and uncertainty. For this reason, different solutions
8 containing varying SRM 981 concentrations (from 100 $\mu\text{g L}^{-1}$ up to 5 mg L^{-1}) were injected in
9 the HPLC system and measured in triplicate. For the sake of simplicity, we have only plotted
10 the results obtained for $^{208}\text{Pb}/^{206}\text{Pb}$ in **Figure 3** but the whole validation dataset can be found in
11 the Supplementary Information (**Figures S2 to S4** and **Tables S1 to S3**). As shown both in
12 **Figure 3** and in the Supplementary Information all results were within the uncertainty of the
13 reference material, with the sole exception of the 100 $\mu\text{g L}^{-1}$ standard, in which the
14 concentration seemed to be too low to obtain accurate results (**Figure S2** and **Table S1**). This
15 effect could be due to the lack of signal-matching between sample and standard or due to a
16 blank contamination. Conversely, the 5 mg L^{-1} solution, 10 times more concentrated than the
17 bracketing standard solution, fitted perfectly within the certified values so there seems to be no
18 need to signal-match samples and standards above a minimum concentration level in the
19 sample.

3.4. Analysis of real samples and comparison with the conventional approach

20
21
22 After method optimisation, 16 archaeological samples containing from 20 $\mu\text{g g}^{-1}$ Pb up to 37%
23 w/w Pb (**Table 2**) were measured in triplicate via HPLC-MC-ICP-MS. The results were
24 compared with those obtained using the conventional off-line separation procedure. A typical
25 chromatogram for one of the more concentrated samples is shown in **Figure 4**. As it can be
26 observed, the Pb peak corresponding to the sample is flanked by the two injections (with the
27 flow injection system) of the NIST 981 for bracketing. The continuous signals correspond to the
28 constant introduction of thallium for mass bias correction and the data points are the point-by-
29 point measurements for the $^{205}\text{Tl}/^{203}\text{Tl}$ isotope ratio. The fact that the thallium isotope ratios
30 follow a constant trend rules out the existence of matrix effects on mass bias during the
31 chromatographic separation.

32
33
34 When comparing the results it was observed that the deviation between both procedures
35 depended on the concentration of Pb in the solid samples. As it can be observed in **Figure 5**,
36 good agreement (relative bias lower than 0.02%) was obtained, both for the ratios $^{207}\text{Pb}/^{206}\text{Pb}$
37 and $^{208}\text{Pb}/^{206}\text{Pb}$, for concentrations higher than 500 $\mu\text{g g}^{-1}$.

38
39
40 The results obtained for the high concentration samples by both approaches are shown in **Table**
41 **5**. As can be seen, there is excellent agreement between the results by both procedures. When
42 compared to the conventional approach, the combined uncertainty for each sample, and Pb ratio,
43
44
45
46
47
48
49
50
51
52
53
54
55
56
57
58
59
60

1
2
3 in the on-line approach increased by a factor of 2-3, depending on the sample and ratio taken
4 into account. This increased uncertainties are due to the transient nature of the signals but are
5 acceptable for the archaeological application described. These capabilities are better seen in
6 **Figure 6** in which the results for the conventional approach are plotted against the on-line
7 results. The nearly perfect line ($r^2 = 0.999$) with slope ≈ 1 reveals that the results for both
8 measurements are comparable. Also, the error bars for each sample show that they are similar
9 by both approaches but, of course, the conventional approach shows better performance figures.
10 Anyway, the differentiation between the archaeological samples is clearly possible by both
11 approaches as shown in **Figure 6**.
12
13
14
15
16
17
18
19

20 **4. Conclusions**

21 The results presented show the suitability of the methodology proposed for samples containing
22 levels of Pb higher than $500 \mu\text{g g}^{-1}$ approximately. Sample preparation time is reduced as no off-
23 line Pb isolation is required. So, this methodology could be a viable alternative for Pb isotope
24 ratio measurements. Unfortunately, for low concentration samples an off-line preconcentration
25 step is still necessary to achieve adequate results. Future work in our laboratory will be focused
26 on the on-line preconcentration of Pb using a cation exchange column together with the
27 proposed chromatographic separation after the elution of Pb from the preconcentration column
28 as anionic EDTA chelate.
29
30
31
32
33
34
35

36 **5. Acknowledgements**

37
38
39 Financial support through grants number PGC2018-097961-B-100 (Agencia Estatal de
40 Investigación) and GRUPIN-IDI/2018/000239 (Fundación para la Investigación Científica y
41 Técnica, FICYT) is gratefully acknowledged.
42
43
44
45
46
47
48
49
50
51
52
53
54
55
56
57
58
59
60

FIGURES

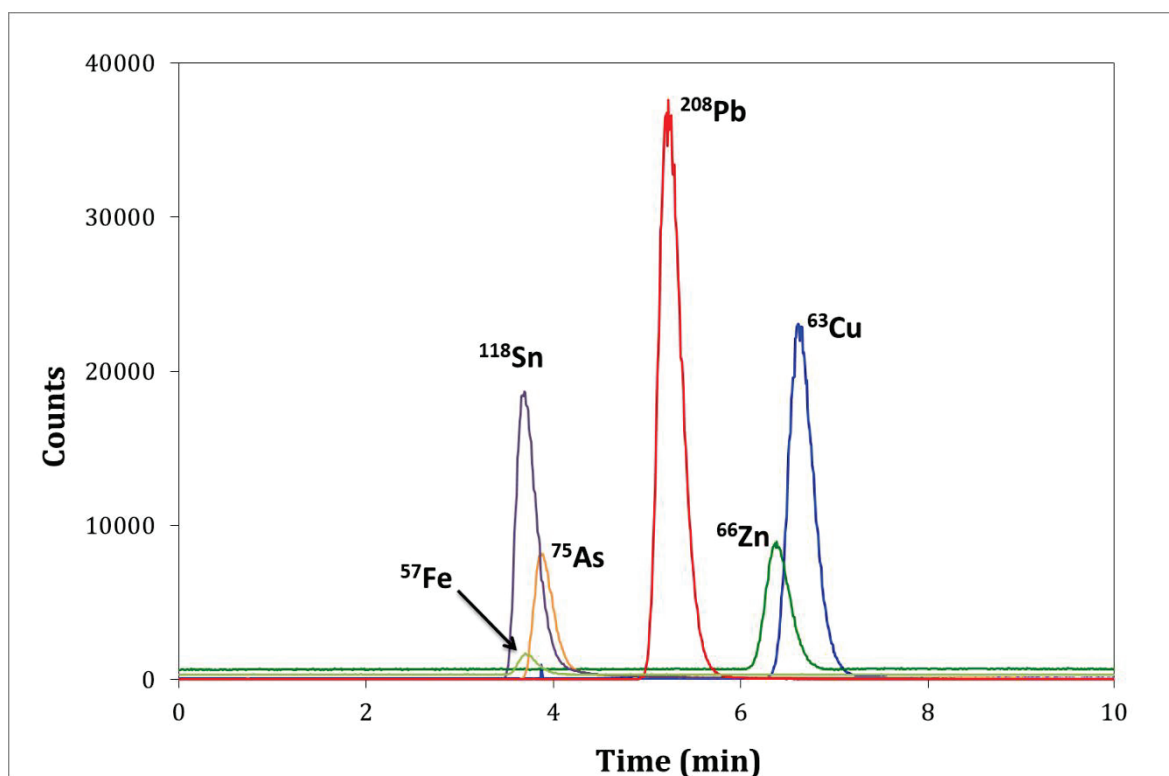


Figure 1: Chromatographic separation of Pb from Sn, As, Cu, Fe and Zn, using a 25 mM $\text{NH}_4\text{NO}_3/5$ mM EDTA mobile phase.

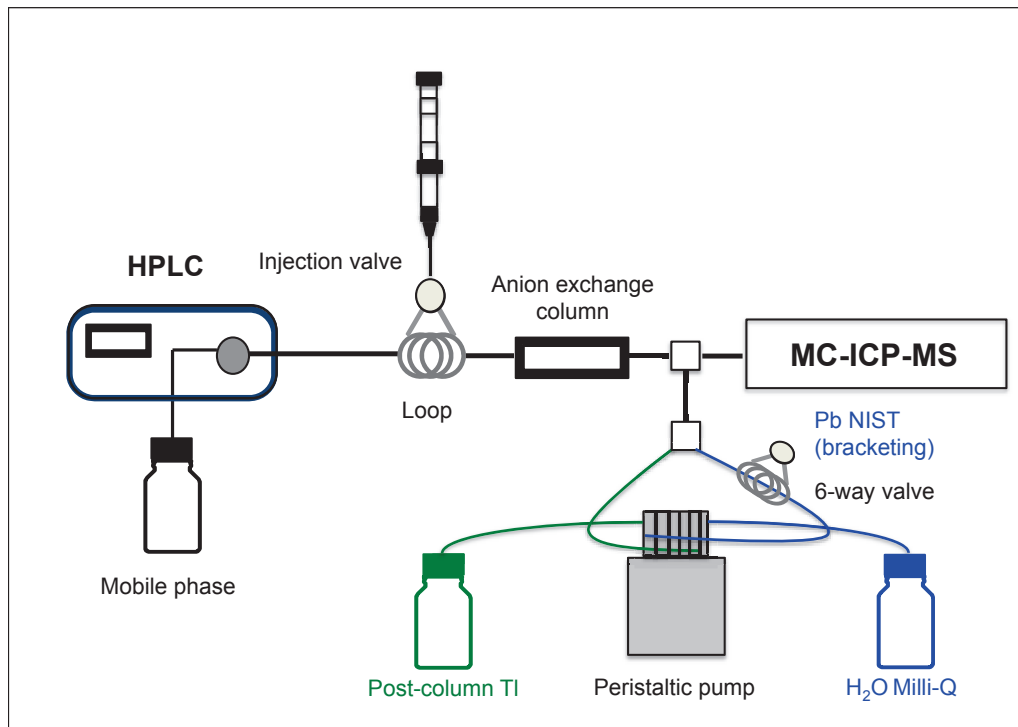


Figure 2: Schematic description of the system to perform the chromatographic separation with the on-line correction.

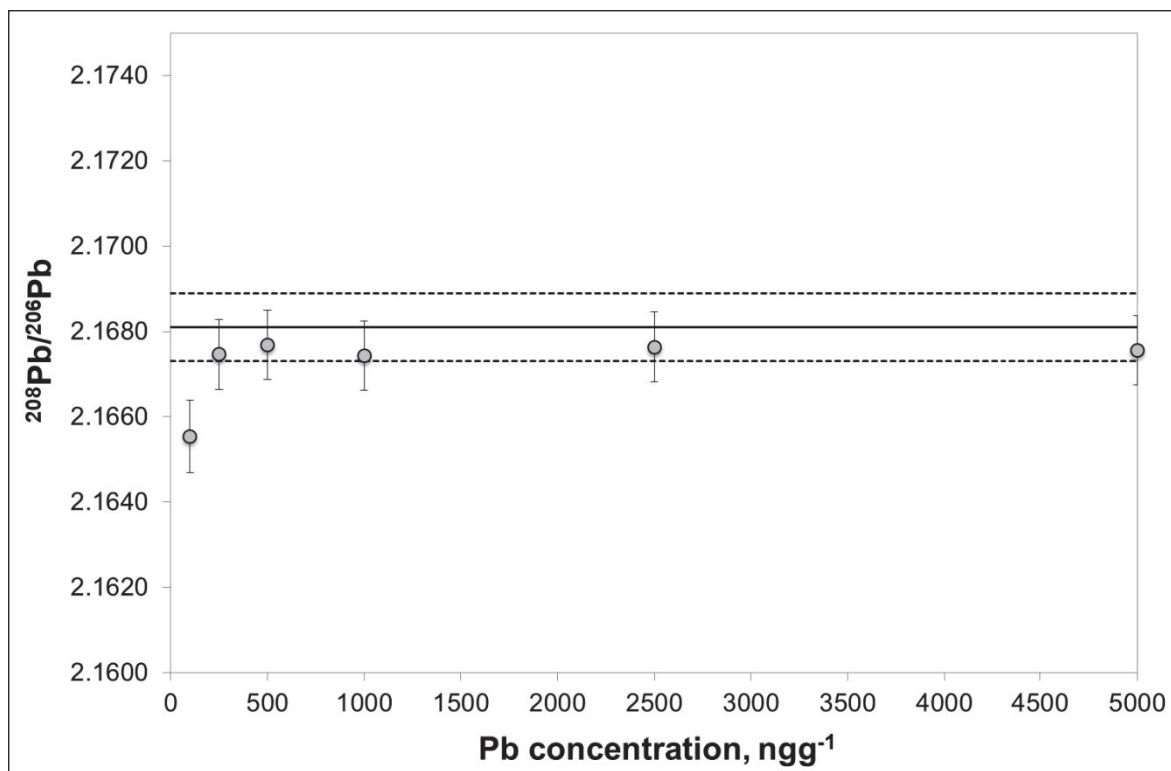


Figure 3: Results for the measurement of $^{208}\text{Pb}/^{206}\text{Pb}$ ratio of SRM 981 at different concentration levels (in triplicate). Error bars correspond to the calculated total combined uncertainties.

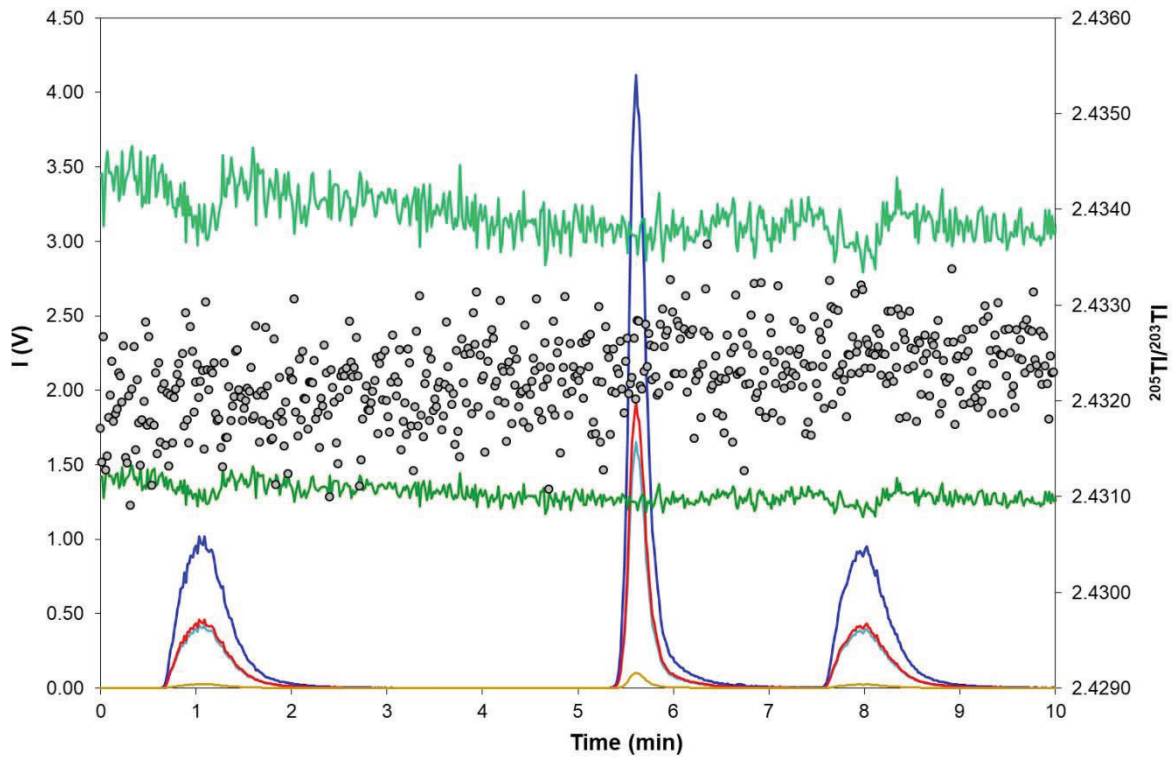


Figure 4: Typical view of a sample chromatogram (AZ 1). Each line corresponds to the different Pb (blue for ^{208}Pb , light blue for ^{207}Pb , red for ^{206}Pb and orange for ^{204}Pb) and Tl (light green for ^{205}Tl and dark green for ^{203}Tl) intensities (left axis); while the dots correspond to the point-by-point $^{205}\text{Tl}/^{203}\text{Tl}$ isotope ratios (right axis).

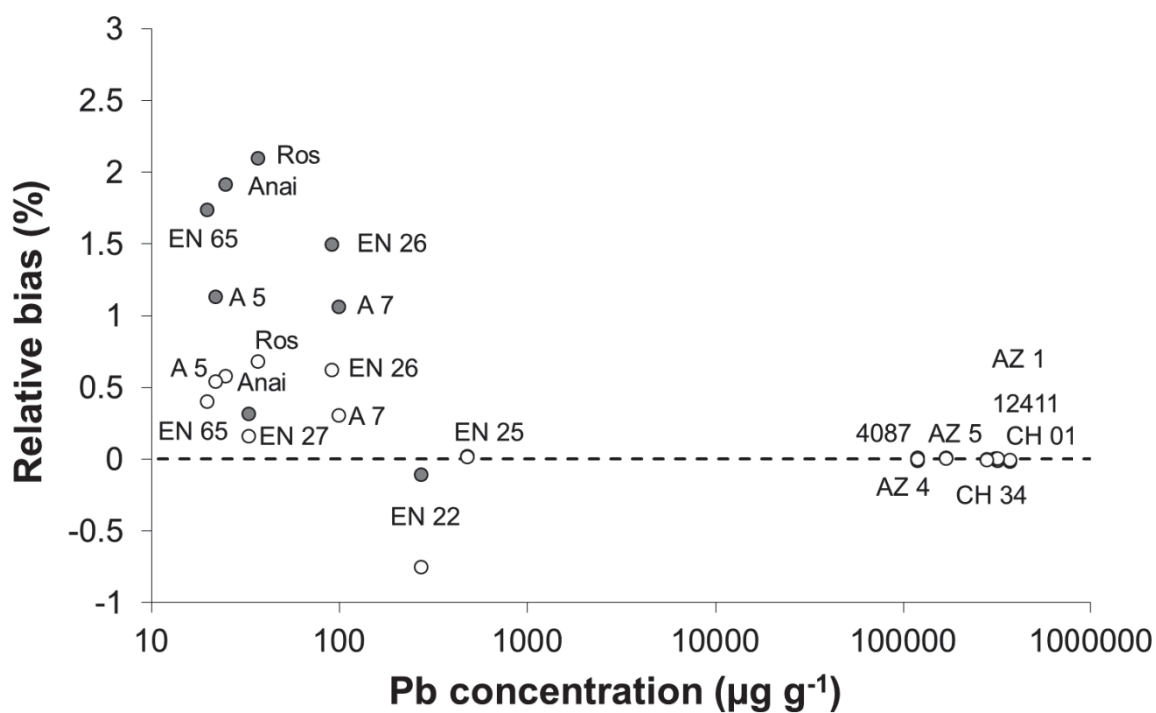
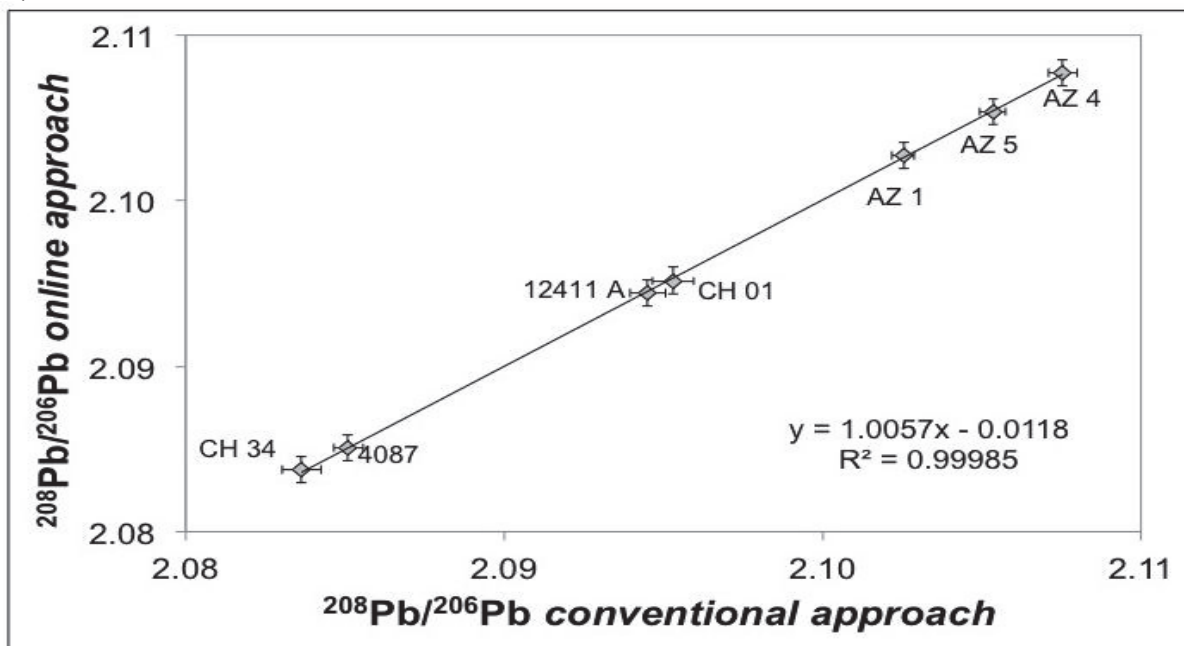


Figure 5. Relative bias in the $^{207}\text{Pb}/^{206}\text{Pb}$ (grey dots) and the $^{208}\text{Pb}/^{206}\text{Pb}$ (white dots) isotope ratios as a function of the concentration of Pb in the solid samples.

A)



B)

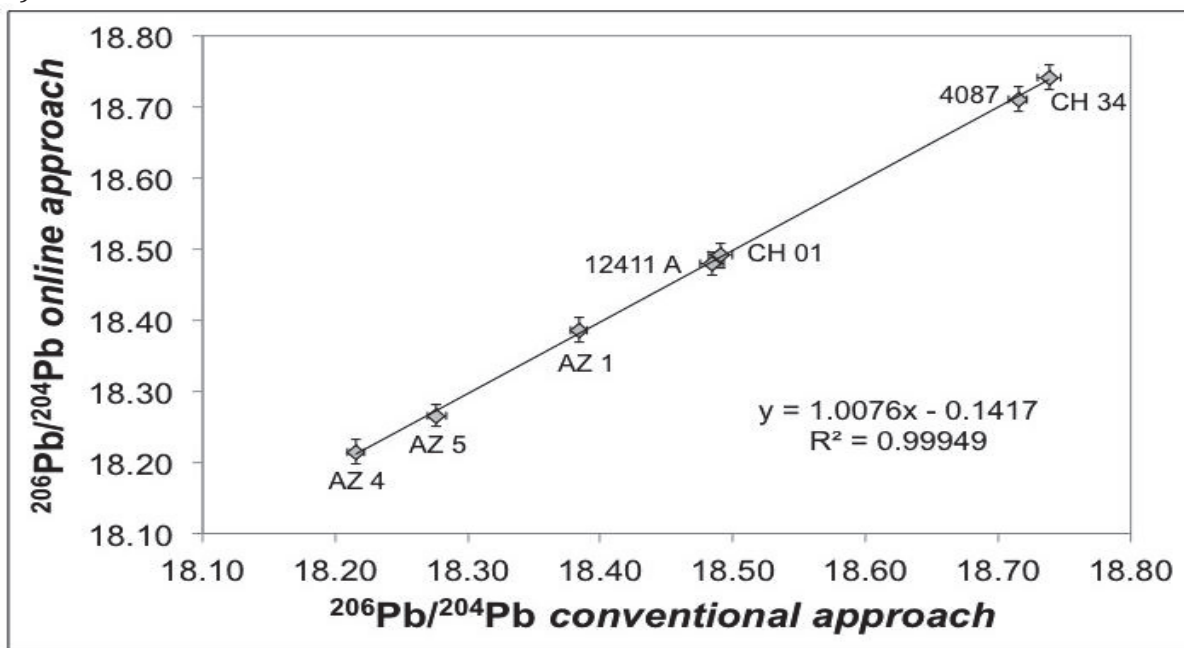


Figure 6: Plot of the results obtained for conventional approach and on-line approach for the $^{208}\text{Pb}/^{206}\text{Pb}$ (A) and $^{206}\text{Pb}/^{204}\text{Pb}$ (B) isotope ratios for the high concentration samples.

TABLES

Table 1: Instrument settings, acquisition parameters and cup configuration used for the measurement in the MC-ICP-MS.

	<i>Conventional approach</i>		<i>Online approach</i>			
Cool gas (L/min)	15.00		15.00			
Auxiliary gas (L/min)	0.85		0.90			
Sample gas (L/min)	1.050		0.990			
Integration time (s)	4.2		1.05			
Number of blocks	1		1			
Cycles per block	50		600			
Mobile phase	---		25 mM NH ₄ NO ₃ /5 mM EDTA			
Flow (mL/min)	---		0.8			
Cup configuration						
L3	L2	L1	C	H1	H2	H3
²⁰² Hg ⁺	²⁰³ Tl ⁺	²⁰⁴ Pb ⁺ , ²⁰⁴ Hg ⁺	²⁰⁵ Tl ⁺	²⁰⁶ Pb ⁺	²⁰⁷ Pb ⁺	²⁰⁸ Pb ⁺

Table 2: Concentrations of Pb in the solid samples and calculated concentrations presented to the instrument for the low concentration samples.

Sample	[Pb] (% w/w)	Sample	[Pb] ($\mu\text{g g}^{-1}$)	Weight taken (mg)	Final Pb concentration (ng g^{-1})
AZ1	31	Anai	25	15.2	38
AZ4	12	Ros	37	20.9	19
AZ5	17	A5	22	28.1	31
CH01	37	A7	100	20.7	104
CH34	32	EN22	275	10.0	137
4087	12	EN25	484	16.6	402
12411	28	EN26	92	35.3	162
		EN27	33	49.3	81
		EN65	20	18.3	18

Table 3: Relative combined uncertainties (%) of the isotope ratios for the triplicate measurement of NIST SRM 981 at the concentration levels and integration times shown. Only mass bias correction using Tl was taken into account for the calculation of the combined uncertainties in the Pb isotope ratios.

Concentration ($\mu\text{g L}^{-1}$)	Integration time (s)	$^{208}\text{Pb}/^{206}\text{Pb}$	$^{207}\text{Pb}/^{206}\text{Pb}$	$^{206}\text{Pb}/^{204}\text{Pb}$	$^{205}\text{Tl}/^{203}\text{Tl}$
250	0.13	0.0064	0.0065	0.0334	0.0042
	0.26	0.0064	0.0070	0.0493	0.0134
	0.52	0.0062	0.0062	0.0423	0.0014
	1.0	0.0051	0.0051	0.0332	0.0033
	2.1	0.0045	0.0049	0.0435	0.0004
	4.2	0.0040	0.0048	0.0355	0.0007
500	0.13	0.0043	0.0054	0.0263	0.0054
	0.26	0.0038	0.0048	0.0248	0.0029
	0.52	0.0038	0.0048	0.0249	0.0011
	1.0	0.0040	0.0051	0.0245	0.0028
	2.1	0.0042	0.0051	0.0282	0.0016
	4.2	0.0040	0.0055	0.0291	0.0008
1000	0.13	0.0051	0.0055	0.0230	0.0049
	0.26	0.0044	0.0054	0.0224	0.0028
	0.52	0.0039	0.0047	0.0226	0.0017
	1.0	0.0039	0.0047	0.0245	0.0030
	2.1	0.0039	0.0047	0.0230	0.0004
	4.2	0.0042	0.0048	0.0241	0.0009

Table 4: Relative combined uncertainties (%) for the measurement (in triplicate) of a Pb NIST 500 ppb/500 ppm Cu with different concentrations for the bracketing and the post-column Tl ($\mu\text{g L}^{-1}$). Combined uncertainties were calculated taken into account the Tl isotope ratios for mass bias correction and the bracketing using the NIST 981 standard, measured both before and after the sample.

Combination ($\mu\text{g L}^{-1}$)	$^{208}\text{Pb}/^{206}\text{Pb}$	$^{207}\text{Pb}/^{206}\text{Pb}$	$^{206}\text{Pb}/^{204}\text{Pb}$	$^{205}\text{Tl}/^{203}\text{Tl}$
Tl 250, Pb 500	0.019	0.028	0.067	0.014
Tl 500, Pb 500	0.022	0.044	0.063	0.014
Tl 1000, Pb 500	0.008	0.007	0.030	0.0009
Tl 500, Pb 250	0.011	0.008	0.034	0.0014
Tl 500, Pb 1000	0.018	0.030	0.062	0.0026

Table 5: Pb isotope ratios obtained for the conventional approach (CA) and for each individual measurement in the on-line approach (OA), and the mean value (Mean OA) of the three replicates. The uncertainty (u_i) for CA and OA is the combined uncertainty of each individual measurement, while for the case of Mean OA is the standard deviation of the replicates. The total combined uncertainty (u_f) for the OA (equation 2) is also shown in the table.

		$^{208}\text{Pb}/^{206}\text{Pb}$	u_x	$^{207}\text{Pb}/^{206}\text{Pb}$	u_x	$^{206}\text{Pb}/^{204}\text{Pb}$	u_x
AZ 1	CA	2.10255	0.00036	0.85181	0.00011	18.3838	0.0062
	OA	2.10266	0.00079	0.85185	0.00031	18.3839	0.0165
		2.10265	0.00079	0.85173	0.00031	18.3799	0.0171
		2.10281	0.00080	0.85182	0.00031	18.3946	0.0168
	Mean OA	2.10271	0.00009	0.85180	0.00006	18.3861	0.0076
u_f (OA)		0.00080		0.00032		0.0174	
AZ 4	CA	2.10755	0.00045	0.85782	0.00012	18.2153	0.0066
	OA	2.10796	0.00079	0.85788	0.00032	18.2164	0.0170
		2.10752	0.00074	0.85797	0.00032	18.2157	0.0168
		2.10769	0.00079	0.85781	0.00031	18.2125	0.0169
	Mean OA	2.10772	0.00022	0.85788	0.00008	18.2149	0.0021
u_f (OA)		0.00079		0.00032		0.0169	
AZ 5	CA	2.10534	0.00043	0.85549	0.00010	18.2765	0.0075
	OA	2.10541	0.00079	0.85558	0.00031	18.2652	0.0162
		2.10539	0.00081	0.85556	0.00033	18.2670	0.0164
		2.10538	0.00079	0.85556	0.00031	18.2668	0.0162
	Mean OA	2.10540	0.00002	0.85557	0.00001	18.2660	0.0010
u_f (OA)		0.00079		0.00031		0.0162	
CH 01	CA	2.09531	0.00065	0.84876	0.00015	18.4904	0.0091
	OA	2.09510	0.00079	0.84856	0.00031	18.4948	0.0169
		2.09514	0.00079	0.84861	0.00031	18.4901	0.0183
		2.09526	0.00079	0.84869	0.00031	18.4877	0.0173
	Mean OA	2.09517	0.00008	0.84862	0.00006	18.4909	0.0036
u_f (OA)		0.00079		0.00031		0.0176	
CH 34	CA	2.08363	0.00062	0.83695	0.00014	18.7382	0.0091
	OA	2.08384	0.00079	0.83698	0.00031	18.7403	0.0172
		2.08365	0.00079	0.83686	0.00031	18.7458	0.0178
		2.08366	0.00079	0.83675	0.00031	18.7393	0.0187
	Mean OA	2.08371	0.00011	0.83686	0.00012	18.7418	0.0035
u_f (OA)		0.00079		0.00032		0.0180	
4087	CA	2.08511	0.00048	0.83805	0.00011	18.7150	0.0067
	OA	2.08504	0.00079	0.83795	0.00031	18.7192	0.0169
		2.08512	0.00079	0.83805	0.00031	18.7086	0.0169
		2.08508	0.00079	0.83794	0.00031	18.7045	0.0170
	Mean OA	2.08508	0.00004	0.83798	0.00006	18.7108	0.0076
u_f (OA)		0.00079		0.00031		0.0175	
12411A	CA	2.09452	0.00055	0.84773	0.00013	18.4843	0.0089
	OA	2.09441	0.00079	0.84764	0.00031	18.4814	0.0165
		2.09429	0.00078	0.84771	0.00031	18.4828	0.0164
		2.09448	0.00078	0.84778	0.00031	18.4760	0.0164
	Mean OA	2.09439	0.00009	0.84771	0.00007	18.4801	0.0036
u_f (OA)		0.00079		0.00031		0.0166	

6. References

- ¹ R. Markey, H. Stein, J. Morgan, Highly precise Re-Os dating for molybdenite using alkaline fusion and NTIMS, *Talanta*, 1998, **45**, 935-946.
- ² R. H. Brill, J. M. Wampler, Isotope studies of ancient lead, *Am. J. Archaeol.*, 1965, **69**, 165-166
- ³ R. H. Brill, J. M. Wampler, Isotope studies of ancient lead, *Am. J. Archaeol.*, 1967, **71**, 63-77.
- ⁴ G. Fortunato, A. Ritter, D. Fabian, Old Masters' lead white pigments: investigations of paintings from the 16th to the 17th century using high precision lead isotope abundance ratios, *Analyst*, 2005, **130**, 898-906.
- ⁵ N. H. Gale, Z. A. Stos-Gale, Bronze Age Copper Sources in the Mediterranean: a new approach, *Science*, 1982, **216**, 11-19.
- ⁶ G. Fortunato, K. Mumic, S. Wunderli, L. Pillonel, J. O. Bosset, G. Gremaud, Application of strontium isotope abundance ratios measured by MC-ICP-MS for food authentication, *J. Anal. At. Spectrom.*, 2004, **19**, 227-234.
- ⁷ S. García-Ruiz, M. Moldovan, G. Fortunato, S. Wunderli, J. I. García Alonso, Evaluation of strontium isotope abundance ratios in combination with multi-elemental analysis as a possible tool to study the geographical origin of ciders, *Anal. Chim. Acta*, 2007, 590, 55-66.
- ⁸ T. Walczyk, F. Von Blanckenburg, Deciphering the iron isotope message of the human body, *Int. J. Mass Spectrom.*, 2005, **242**, 117-134.
- ⁹ M. Costas-Rodríguez, Y. Anoshkina, S. Lauwens, H. Van Vlierberghe, J. Delanghe, F. Vanhaecke, Isotopic analysis of Cu in blood serum by multi-collector ICP-mass spectrometry: a new approach for the diagnosis and prognosis of liver cirrhosis? *Metallomics*, 2015, **7**, 491-498.
- ¹⁰ C. Cloquet, J. Carignan, G. Libourel, Atmospheric pollutant dispersal around an urban area using trace metal concentrations and Pb isotopic compositions in epiphytic lichens, *Atmos. Environ.*, 2006, **40**, 574-587.
- ¹¹ L. Yang, E. Dabek-Zlotorzynska, V. Celo, High precision determination of silver isotope ratios in commercial products by MC-ICP-MS, *J. Anal. At. Spectrom.*, 2009, **24**, 1564-1569.

-
- 1
2
3
4 ¹² J. Meija, T. B. Coplen, M. Berglund, W. A. Brand, P. De Bièvre, M. Gröning, N. E.
5 Holden, J. Irrgeher, R. D. Loss, T. Walczyk, T. Prohaska, Isotopic compositions of the
6 elements 2013 (IUPAC Technical Report), *Pure Appl. Chem.*, 2016, **88 (3)**, 293-306.
7
8 ¹³ C. B. Douthitt, *Anal. Bioanal. Chem.*, 2008, **390**, 437-440.
9
10 ¹⁴ D. De Muynck, C. Cloquet, F. Vanhaecke, *J. Anal. At. Spectrom.*, 2008, **23**, 62-71
11
12
13 ¹⁵ C. N. Maréchal, P. Télouk, F. Albarède, Precise analysis of copper and zinc
14 isotopic compositions by plasma-source mass spectrometry, *J. Anal. At. Spectrom.*,
15 1999, **156**, 251-273.
16
17
18 ¹⁶ S. García-Ruiz, M. Moldovan, J. I. García Alonso, Measurement of strontium
19 isotope ratios by MC-ICP-MS after on-line Rb-Sr ion chromatography separation, *J.*
20 *Anal. At. Spectrom.*, 2008, **23 (1)**, 84-93.
21
22
23 ¹⁷ I. Günther-Leopold, B. Wernli, Z. Kopajtic, D. Günther, Measurement of isotope
24 ratios on transient signals by MC-ICP-MS, *Anal. Bioanal. Chem.*, 2004, **378**, 241-
25 249.
26
27
28 ¹⁸ T. Hirata, Y. Hayano, T. Ohno, Improvements in precision of isotopic ratio
29 measurements using laser-ablation multiple collector-ICP-mass spectrometry:
30 reduction of changes in measured isotopic ratios, *J. Anal. At. Spectrom.*, 2003, **18**,
31 1283-1288.
32
33
34 ¹⁹ E. M. Krupp, O. F. X. Donard, Isotope ratios on transient signals with GC-MC-ICP-
35 MS, *Int. J. Mass Spectrom.*, 2005, **242**, 233-242.
36
37
38 ²⁰ B. Martelat, L. Vio, H. Isnard, J. Simonnet, T. Cornet, A. Nonell, F. Chartier,
39 Neodymium isotope ratio measurements by CE-MC-ICPMS: investigation of
40 isotopic fractionation and evaluation of analytical performances, *J. Anal. At.*
41 *Spectrom.*, 2017, **32**, 2271-2280.
42
43
44 ²¹ F. Guéguen, H. Isnard, A. Nonell, L. Vio, T. Vercoüter, F. Chartier, Neodymium
45 isotope ratio measurements by LC-MC-ICPMS for nuclear applications:
46 investigation of isotopic fractionation and mass bias correction, *J. Anal. At.*
47 *Spectrom.*, 2015, **30**, 443-452.
48
49
50 ²² M. Martinez, J. I. García Alonso, C. Parat, J. Ruiz Encinar, I. Le Hécho, Anion-
51 Specific Sulfur Isotope Analysis by Liquid Chromatography Coupled to
52 Multicollector ICPMS, *Anal. Chem.*, 2019, **91**, 10088-10094.
53
54
55
56
57
58
59
60

1
2
3
4
5
6
7
8
9
10
11
12
13
14
15
16
17
18
19
20
21
22
23
24
25
26
27
28
29
30
31
32
33
34
35
36
37
38
39
40
41
42
43
44
45
46
47
48
49
50
51
52
53
54
55
56
57
58
59
60

²³ M. K. Ullrich, F. Gelman, Y. Zakon, L. Halicz, K. Knöller, B. Planer-Friedrich, Sulfur isotope analysis by IC-MC-ICP-MS provides insight into fractionation of thioarsenates during abiotic oxidation, *Chem. Geol.*, 2018, **477**, 92-99.

²⁴ Y Zakon, L. Halicz, F. Gelman, Isotope Analysis of Sulfur, Bromine, and Chlorine in Individual Anionic Species by Ion Chromatography/Multicollector-ICPMS, *Anal. Chem.*, 2014, **86**, 6495-6500.

²⁵ J. Fietzke, V. Liebetrau, D. Günther, K. Gürs, K. Hametner, K. Zumholz, T. H. Hansteen, A. Eisenhauer, An alternative data acquisition and evaluation strategy for improved isotope ratio precision using LA-MC-ICP-MS applied to stable and radiogenic strontium isotopes in carbonates, *J. Anal. At. Spectrom.*, 2008, **23**, 955-961.

²⁶ J. A. Rodríguez-Castrillón, S. García-Ruíz, M. Moldovan, J. I. García Alonso, Multiple linear regression and on-line ion exchange chromatography for alternative Rb-Sr and Nd-Sm MC-ICP-MS isotopic measurements, *J. Anal. At. Spectrom.*, 2012, **27**, 611-618.

²⁷ J. A. Cuchí-Oterino, P. Alvarez Penanes; J. Martín-Gil, M. Moldovan, I. Aguilera Aragón, P. Martín-Ramos, Mineral provenance of Roman lead objects from the Cinca River basin (Huesca, Spain), *J. Archaeol. Sci. Rep.*, 2021, submitted.

²⁸ A. Reguera-Galán, T. Barreiro-Grille, M. Moldovan, L. Lobo, M. A. De Blas Cortina, J. I. García Alonso, A provenance study of early Bronze Age artefacts found in Asturias (Spain) by means of metal impurities and lead, copper and antimony isotopic compositions, *Archaeometry*, 2018, **61 (3)**, 683-700.

²⁹ R. García Fernández, J. I. García Alonso, Separation of rare earth elements by anion-exchange chromatography using ethylenediaminetetraacetic acid as mobile phase, *J. Chrom. A*, 2008, **1180**, 59-65.

³⁰ S. Queipo-Abad, P. Rodríguez-González, J. I. García Alonso, Measurement of compound-specific Hg isotopic composition in narrow transient signals by gas chromatography coupled to multicollector ICP-MS, *J. Anal. At. Spectrom.*, 2019, **34**, 753-763.

³¹ L. Yang, Accurate and precise determination of isotopic ratios by MC-ICP-MS: a review, *Mass Spectrom. Rev.*, 2009, **28**, 990-1011